Differential scattering and rethermalization in ultracold dipolar gases

John L. Bohn* and Deborah S. Jin

JILA, NIST, and Department of Physics, University of Colorado Boulder, Boulder, Colorado 80309, USA

(Received 10 December 2013; revised manuscript received 17 January 2014; published 5 February 2014)

Analytic expressions for the differential cross sections of ultracold atoms and molecules that scatter primarily due to dipolar interactions are derived within the first-order Born approximation and are shown to agree with the partial wave expansion. These cross sections are applied to the problem of cross-dimensional rethermalization. Strikingly, the rate of rethermalization can vary by as much as a factor of 2, depending on the orientation of the dipoles. Thus the anisotropic dipole-dipole interaction can have a significant effect even on the behavior of a nondegenerate ultracold gas.

DOI: 10.1103/PhysRevA.89.022702 PACS number(s): 34.50.Cx, 67.85.−d

I. INTRODUCTION

It is commonly appreciated that the ultracold regime of collisions occurs when only a small number of partial waves contributes to scattering. This is a sensible criterion for atoms interacting via van der Waals forces, where the Wigner threshold laws dictate that scattering amplitudes are independent of wave number k for s-wave collisions (and represented by a scattering length) but that they diminish as higher powers of k for higher partial waves [1]. For atoms or molecules scattering via dipolar forces, however, this criterion fails, since the threshold scattering amplitude for *all* nonzero partial waves is independent of k [2]. Thus, in principle, a large number of partial waves may be necessary to describe scattering of polar species even in the zero-temperature limit.

It is therefore worthwhile to describe the scattering of polar species directly in coordinate space, rather than in terms of angular momentum quantum numbers. The effective range expansion for scattering in the appropriate potential has been known for some time [3,4]. In the threshold limit, it presents a leading-order scattering amplitude that depends on the direction of both incident and outgoing momenta and that is independent of the magnitude k. In this paper we focus on this leading-order term, rederiving it in the first-order Born approximation and expressing it in a coordinate-independent way, for both identical bosons and identical fermions. Further, we make explicit the relation between the coordinate-space version and the partial-wave-expansion version of the cross section. Significantly, we identify a formal discontinuity in the scattering amplitude for forward scattering, which may render the partial-wave expansion slow to converge numerically.

We illustrate the influence of the anisotropy of scattering by using it to calculate the rate of rethermalization in a classical gas that has been brought out of thermal equilibrium. While dipole interactions are now well known to influence the behavior of quantum degenerate Bose gases [5], we illustrate here a significant effect of the anisotropy of collision in a thermal (but still ultracold) gas. These results have implications for collisions and, especially, for evaporative cooling of polar molecules or highly magnetic atoms such as dysprosium [6,7] and erbium [8,9].

II. CROSS SECTIONS

For the sake of concreteness, we speak of polar molecules polarized in an electric field $\mathcal{E}$, although the results apply equally to magnetic atoms polarized in a magnetic field. These molecules interact via the dipole potential (in CGS units):

$$V_d(\mathbf{r}) = \frac{\mathbf{d}_1\cdot\mathbf{d}_2 - 3(\hat{r}\cdot\mathbf{d}_1)(\hat{r}\cdot\mathbf{d}_2)}{r^3} = -\frac{2d^2}{r^3}C_{20}(\theta,\phi). \quad (1)$$

Here $\mathbf{d}_{1,2}$ are the molecular dipole moments, $\mathbf{r}$ is the relative coordinate joining them, and $C_{20} = (3\cos^2\theta - 1)/2$ is a reduced spherical harmonic [10]. Writing the interaction in this way assumes that the electric-field direction coincides with the laboratory z axis. This orientation simplifies the derivation of the cross section, but subsequently the cross section will be cast in a coordinate-independent form. In the final expression on the right-hand side of (1) we employ a single dipole moment d as if the molecules were the same. More generally, the replacement $d^2 \to d_1 d_2$ can be made, if the dipoles are different.

The Hamiltonian describing scattering of the molecules, in their center-of-mass frame, is

$$H = -\frac{\hbar^2}{2\mu}\vec{\nabla}^2 + V_d + V_{\rm sr}, \quad (2)$$

where, as usual, μ stands for the reduced mass of the collision partners. In (2) we allow for an additional short-range interaction $V_{\rm sr}$ that can describe an s-wave phase shift not already accounted for by the dipole potential. It is convenient to convert the scattering problem into dipole units, where the natural length and energy scales are, respectively,

$$a_d = \frac{\mu d^2}{\hbar^2}, \quad E_d = \frac{\hbar^6}{\mu^3 d^4}. \quad (3)$$

Cast in these units, the Schrödinger equation reads

$$\left[-\frac{1}{2}\vec{\nabla}^2 - \frac{2C_{20}}{r^3} + V_{\rm sr}\right]\psi = \epsilon\psi, \quad (4)$$

where $\epsilon = (\hbar^2k^2/2\mu)/E_d$ is the collision energy in reduced units.

*bohn@murphy.colorado.edu

A. Scattering amplitudes

Scattering in three dimensions is characterized by a differential cross section that relates the wave vector $\mathbf{k}$ of the molecules' initial approach to one another to the wave vector $\mathbf{k}'$ into which they scatter,

$$\frac{d\sigma}{d\Omega_{\mathbf{k}'}}(\mathbf{k}',\mathbf{k}) = |f(\mathbf{k}',\mathbf{k})|^2, \tag{5}$$

written, as is conventional, in terms of a scattering amplitude f. The total scattering cross section is then

$$\sigma(\mathbf{k}) = \int d\Omega_{\mathbf{k}'} \frac{d\sigma}{d\Omega_{\mathbf{k}'}}(\mathbf{k}',\mathbf{k}), \tag{6}$$

which for dipoles can depend on the orientation of the incident direction $\mathbf{k}$ with respect to the polarization axis.

In the case of indistinguishable bosons or fermions, symmetry places constraints on the scattering amplitudes. Specifically, the amplitude for scattering from a given incident direction $\mathbf{k}$ must be properly symmetrized with respect to two opposing scattering directions $\pm\mathbf{k}'$:

$$f_{B,F}(\mathbf{k}',\mathbf{k}) = \frac{1}{\sqrt{2}}[f(\mathbf{k}',\mathbf{k}) \pm f(-\mathbf{k}',\mathbf{k})]. \tag{7}$$

The resulting cross sections are then [11]

$$\sigma_{B,F} = \int d\Omega_{\mathbf{k}'} |f_{B,F}(\mathbf{k}',\mathbf{k})|^2. \tag{8}$$

We stress again that we work in reduced units. To restore the results to "real" units, one must multiply f by the dipole length a_d, and σ by a_d^2.

B. Cross-section formulas

The dipole-dipole interaction in Eq. (4) is mathematically identical to the leading-order long-range potential between an electron and a molecule possessing a nonzero quadrupole moment. In this context, the low-energy scattering in such a potential has been worked out previously, including several orders of the effective range expansion [3,4]. For our present purposes, considering ultracold collisions, we require only the leading-order term in these expansions. Indeed, the first-order term can be obtained in perturbation theory, which derivation we include here for completeness.

The scattering amplitude is given, within the first-order Born approximation, by

$$f(\mathbf{k}',\mathbf{k}) = -a + f^{(1)}(\mathbf{k}',\mathbf{k}), \tag{9}$$

where a is the s-wave scattering length in units of a_d (recalling that the nondipolar scattering amplitude is $f = -a/(1+iak) \approx -a$ [12], and $f^{(1)}$ denotes the first-order Born approximation for dipolar scattering [13]):

$$f^{(1)}(\mathbf{k}',\mathbf{k}) = -\frac{1}{2\pi}\int d^3r e^{-i\mathbf{k}'\cdot\mathbf{r}} V_d(\mathbf{r}) e^{i\mathbf{k}\cdot\mathbf{r}}. \tag{10}$$

As is typical for the first-order Born approximation, the scattering amplitude depends only on the momentum transfer,

$$\mathbf{q} = \mathbf{k} - \mathbf{k}', \tag{11}$$

and not on the incoming and outgoing amplitudes separately. To evaluate the integral, (10), we expand $e^{i\mathbf{q}\cdot\mathbf{r}}$ into spherical waves, to get

$$\begin{aligned} f^{(1)}(\mathbf{k}',\mathbf{k}) &= -\frac{1}{2\pi}\int d^3r \left(-\frac{2C_{20}(\hat{r})}{r^3}\right) e^{i\mathbf{q}\cdot\mathbf{r}} \\ &= \frac{1}{\pi}\int d^3r \frac{C_{20}(\hat{r})}{r^3} 4\pi \sum_{lm} i^l Y_{lm}^*(\hat{q}) j_l(qr) Y_{lm}(\hat{r}), \end{aligned} \tag{12}$$

where Y_{lm} is the usual spherical harmonic, and j_l is a spherical Bessel function. Inside this sum, the angular integral is

$$\int d\hat{r} C_{20}(\hat{r}) Y_{lm}(\hat{r}) = \sqrt{\frac{4\pi}{5}}\delta_{2l}\delta_{0m}, \tag{13}$$

which reduces the sum to a single term. The relevant radial integral is then

$$\begin{aligned} \int_0^\infty r^2 dr \frac{j_2(qr)}{r^3} &= \lim_{b\to 0}\int_b^\infty dr \frac{j_2(qr)}{r} \\ &= \lim_{b\to 0}\left[\frac{\sin(qb)}{(qb)^3} - \frac{\cos(qb)}{(qb)^2}\right] = \frac{1}{3}. \end{aligned} \tag{14}$$

Substituting this integral, the Born approximation to the scattering amplitude becomes [3,4,14]

$$f^{(1)}(\mathbf{k}',\mathbf{k}) = -\tfrac{2}{3}(3\cos^2\theta_q - 1), \tag{15}$$

where θ_q is the angle between the momentum transfer $\mathbf{q}$ and the z axis.

The scattering amplitude can also be written in terms of the incident and scattered wave numbers, as well as the direction $\hat{\mathcal{E}}$ of the electric field (taking this to be the z axis) [3]:

$$\cos^2\theta_q = \frac{q_z^2}{|\mathbf{q}|^2} = \frac{1}{2}\frac{(\hat{k}\cdot\hat{\mathcal{E}} - \hat{k}'\cdot\hat{\mathcal{E}})^2}{1-\hat{k}\cdot\hat{k}'}. \tag{16}$$

This expression assumes elastic scattering, $k' = k$. Doing so re-expresses the scattering amplitude in the coordinate-free form:

$$f(\mathbf{k}',\mathbf{k}) = -a - \frac{(\hat{k}\cdot\hat{\mathcal{E}} - \hat{k}'\cdot\hat{\mathcal{E}})^2}{1-\hat{k}\cdot\hat{k}'} + \frac{2}{3}. \tag{17}$$

Using the prescriptions above, this leads immediately to the scattering amplitudes for antisymmetrized and symmetrized scattering amplitudes, here denoted by the subscript F (fermion) and B (boson), respectively:

$$\begin{aligned} f_F(\mathbf{k}',\mathbf{k}) &= \frac{1}{\sqrt{2}}\frac{4(\hat{k}\cdot\hat{\mathcal{E}})(\hat{k}'\cdot\hat{\mathcal{E}}) - 2[(\hat{k}\cdot\hat{\mathcal{E}})^2 + (\hat{k}'\cdot\hat{\mathcal{E}})^2](\hat{k}\cdot\hat{k}')}{1-(\hat{k}\cdot\hat{k}')^2}, \\ f_B(\mathbf{k}',\mathbf{k}) &= \frac{1}{\sqrt{2}}\left[-2a - \frac{2(\hat{k}\cdot\hat{\mathcal{E}})^2 + 2(\hat{k}'\cdot\hat{\mathcal{E}})^2 - 4(\hat{k}\cdot\hat{\mathcal{E}})(\hat{k}'\cdot\hat{\mathcal{E}})(\hat{k}\cdot\hat{k}')}{1-(\hat{k}\cdot\hat{k}')^2} + \frac{4}{3}\right]. \end{aligned} \tag{18}$$

These are expressed in units of the dipole length a_d and depend only on the directions of the momenta, not their magnitudes. The angular dependence of these cross sections will have significant implications for the redistribution of kinetic energy in a gas brought out of equilibrium, as we see below.

C. Dependence of scattering on incident direction

Because of the anisotropic nature of dipole-dipole scattering, and because of the fixed direction in space set by the electric field $\mathcal{E}$, the total scattering cross sections is also a function of the incident direction. The cross section remains cylindrically symmetric around the field axis and is therefore a function of the angle $\eta = \cos^{-1}(\hat{k}\cdot\hat{\mathcal{E}})$ between the incident wave vector and the polarization axis:

$$\sigma(\eta) = \int d\Omega_{\mathbf{k}'} \frac{d\sigma}{d\Omega_{\mathbf{k}'}}. \tag{19}$$

To evaluate these integrals it is convenient to choose a coordinate system whose z axis coincides with the incident direction $\hat{k}$. The electric-field direction is then rotated into the x-z plane of this system, with $\hat{\mathcal{E}} = (-\sin\eta, 0, \cos\eta)$. In this coordinate system, the spherical coordinates of $\hat{k}'$ constitute the scattering angles (θ_s, ϕ_s). Then, for example, the cross section for the unsymmeterized scattering amplitude is

$$\begin{aligned}\sigma(\eta) &= \int_0^{2\pi} d\phi_s \int_0^{\pi} \sin\theta_s d\theta_s \left[-a - \frac{[\cos\eta(1-\cos\theta_s) + \sin\eta\sin\theta_s\cos\phi_s]^2}{1-\cos\theta_s} + \frac{2}{3}\right]^2 \\ &= \frac{2\pi}{9}[18a^2 - 3a(2-6\cos^2\eta) + 5 + 6\cos^2\eta - 3\cos^4\eta].\end{aligned} \tag{20}$$

This result is cylindrically symmetric about the electric-field axis. It is also convenient to define an angular average of the cross section [4],

$$\bar{\sigma} = \frac{1}{2}\int_{-1}^{+1} d(\cos\eta)\sigma(\eta) \tag{21}$$

$$= 4\pi a^2 + \frac{64\pi}{45}, \tag{22}$$

where the bar is meant here to denote the average over an assumed isotropic distribution of incident directions. Here the first term is the usual, nondipolar, s-wave cross section. The second term is the pure dipolar result and is implicitly multiplied by the square of the dipole length a_d. Note that this result, $64\pi/45 \approx 1.117 + 3.351$, gives the sum of the even and odd partial-wave contributions, respectively, as calculated from close-coupling calculations in Ref. [15].

Similarly, the total cross section for indistinguishable fermions, as a function of η, is

$$\sigma_F = \frac{\pi}{3}[3 + 18\cos^2(\eta) - 13\cos^4(\eta)], \tag{23}$$

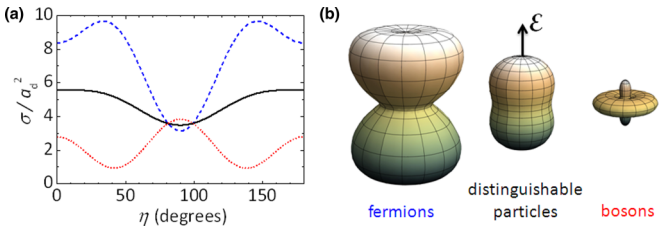

FIG. 1. (Color online) (a) Total cross section $\bar{\sigma}$ for pure dipolar scattering, as a function of the angle η between the incident direction and the polarizing electric field. The solid black line is for distinguishable particles, while the dashed (blue) and dotted (red) lines represent indistinguishable fermions and bosons, respectively. (b) The same data, shown as three-dimensional plots.

with angular average

$$\bar{\sigma}_F = \frac{32\pi}{15}; \tag{24}$$

and the total cross section for indistinguishable bosons is

$$\begin{aligned}\sigma_B = \frac{\pi}{9}\{&[72a^2 - 24a[(1-3\cos^2(\eta)] \\ &+ 11 - 30\cos^2(\eta) + 27\cos^4(\eta)\},\end{aligned} \tag{25}$$

with angular average

$$\bar{\sigma}_B = 8\pi a^2 + \frac{32\pi}{45}. \tag{26}$$

These total cross sections are depicted in Fig. 1, shown to the same scale. This figure reveals that dipolar fermions scatter more strongly than dipolar bosons. Whereas bosons scatter most readily when they meet side by side, fermions tend to scatter most when meeting at an angle $\eta \approx 45^{\circ}$ with respect to the field axis.

III. CROSS-DIMENSIONAL RETHERMALIZATION

An essential effect of elastic collisions for ultracold gas experiments is the thermalization of the gas, for example, during evaporative cooling. Turning this around, measurements of rethermalization rates can be used as an experimental tool for extracting the elastic collision cross section, which is a key ingredient to understanding and designing ultracold gas experiments. Here we point out an important effect on thermalization via dipolar elastic collisions that follows from the anisotropy of dipolar interactions. Dipolar collisions depend not only on the scattering angle (i.e., the angle between $\mathbf{k}$ and $\mathbf{k}'$), but also on the quantization direction set by the electric-field direction $\hat{\mathcal{E}}$. At the same time, traps for ultracold gases have principal axes that define a relevant coordinate system in space (which is often aligned with the Earth's gravitational field) and thermalization must include cross-dimensional thermalization, i.e., keeping the energy in the different trap directions equilibrated. The axes of equilibration

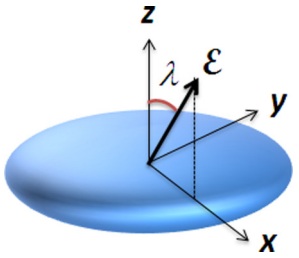

FIG. 2. (Color online) Geometry of a cross-dimensional rethermalization experiment. A cylindrically symmetric cloud, with symmetry axis $\hat{z}$, is driven out of equilibrium, giving it either more or less average kinetic energy in the axial direction than in the radial direction. The rate of rethermalization is, in general, a function of the angle λ between the symmetry axis and the electric or magnetic field that polarizes the dipoles.

are shown schematically in Fig. 2. A consequence of this is that the orientation of the quantization direction with respect to the trap axes, described by the angle λ, can strongly affect thermalization rates.

A. Rethermalization rate

The idea of a rethermalization experiment is to preferentially add or remove energy along one direction of the trapped gas, then observe the energies in the different trap directions come to equilibrium through elastic collisions [16]. Fitting the energy in a particular trap direction versus time to an exponential, one finds a rethermalization time τ or, equivalently, rethermalization rate $\gamma = 1/\tau$. From this, one extracts a rethermalization cross section defined by

$$\gamma = n v_r \sigma_{\text{retherm}}, \tag{27}$$

in terms of the average number density $n = (1/N)\int d^3r n(\mathbf{r})^2$ and the mean relative speed $v_r = \sqrt{8k_BT/\pi\mu}$, which are empirically determined quantities. Here N is the total number of particles, k_B is Boltzmann's constant, μ is the reduced mass, and T is the temperature of the gas.

The cross section σ_{retherm} extracted from rethermalization data is not, in general, identical to the average total cross section $\bar{\sigma}$, but the two are proportional:

$$\bar{\sigma} = \alpha \sigma_{\text{retherm}}. \tag{28}$$

The constant of proportionality α, described by theory, allows one to extract the mean cross section from rethermalization measurements. It can be interpreted as the ratio of a standard collision rate $n v_r \bar{\sigma}$ to the rethermalization rate γ and is often colloquially referred to as the "number of collisions per rethermalization," even though it need not take integer values. For s-wave collisions $\alpha = 2.5$, whereas for p-wave collisions $\alpha = 4.17$ [17]. The larger value of α for p-wave scattering arises from the fact the p-wave scattering occurs preferentially in the forward and backward scattering directions and is thus less efficient at rethermalization than isotropic s-wave scattering. For dipoles, α will in general be a function of the electric-field direction λ.

In the experiment, the trapping potential can be parametrically driven in a certain direction, say the z direction, leading to an effective temperature T_z that is higher than the effective temperature T_y in the other two directions (T_y could also be made the higher one, of course). The temperatures are to be interpreted as parameters in the quasiequilibrium phase-space distribution,

$$\frac{d^6N}{d^3r d^3v}(\mathbf{r},\mathbf{v};\mathbf{T}) = n(\mathbf{r},\mathbf{T})\rho(\mathbf{v},\mathbf{T}), \tag{29}$$

which is given in terms of the space and velocity densities,

$$n(\mathbf{r},\mathbf{T}) = N\Pi_{i=x,y,z}\left(\frac{m\omega_i^2}{2\pi k_B T_i}\right)^{1/2}\exp\left[-\frac{1}{2}\frac{m\omega_i^2 r_i^2}{k_B T_i}\right],$$
$$\rho(\mathbf{v},\mathbf{T}) = \Pi_{i=x,y,z}\left(\frac{m}{2\pi k_B T_i}\right)^{1/2}\exp\left[-\frac{1}{2}\frac{m v_i^2}{k_B T_i}\right]. \tag{30}$$

Here the notation $\mathbf{T} = (T_x, T_y, T_z)$ parametrizes the temperatures in the different directions. This distribution is normalized so that its integral over all phase space is equal to N, the total number of molecules.

Bringing the gas out of equilibrium introduces a disparity between the mean energy per particle in the vertical and that in the horizontal direction, defined by

$$\langle\chi\rangle \equiv \frac{1}{N}\left\langle\left(\frac{1}{2}m\omega^2 z^2 + \tfrac{1}{2}m v_z^2\right) - \left(\frac{1}{2}m\omega^2 y^2 + \frac{1}{2}m v_y^2\right)\right\rangle$$
$$= k_B(T_z - T_y), \tag{31}$$

where the angle brackets indicate averaging over the distribution in Eq. (30). The value of $\langle\chi\rangle$ relaxes to 0 via collisions involving a pair of molecules with velocities $\mathbf{v}_1$ and $\mathbf{v}_2$. After a collision that changes the velocities to the values $\mathbf{v}_1'$ and $\mathbf{v}_2'$, χ changes by the amount [18]

$$\Delta\chi = \chi(\mathbf{v}_1') + \chi(\mathbf{v}_2') - \chi(\mathbf{v}_1) - \chi(\mathbf{v}_2)$$
$$= \tfrac{1}{2}m\left(v_{1z}'^2 - v_{1y}'^2 + v_{2z}'^2 - v_{2y}'^2\right)$$
$$- \tfrac{1}{2}m\left(v_{1z}^2 - v_{1y}^2 + v_{2z}^2 - v_{2y}^2\right). \tag{32}$$

In this expression the potential energies before and after the collision cancel, since the collision occurs at a particular location in the trap. The time evolution of $\langle\chi\rangle$ is given by the Enskog equation [18],

$$\frac{d\langle\chi\rangle}{dt} = C(\Delta\chi), \tag{33}$$

in terms of the collision integral (also per particle)

$$C(\Delta\chi) = \frac{1}{2N}\int d^3r_1\int d^3v_1\int d^3r_2\int d^3v_2\frac{d^6N}{d^3r_1 d^3v_1}\frac{d^6N}{d^3r_2 d^3v_2}\delta(\mathbf{r}_1 - \mathbf{r}_2)\int d\Omega_{\mathbf{k}'}\frac{d\sigma}{d\Omega_{\mathbf{k}'}}|\mathbf{v}_1 - \mathbf{v}_2|\Delta\chi. \tag{34}$$

The collision integral simplifies by separating the space- and velocity-dependent parts and by representing velocities in terms of the center-of-mass velocity $\mathbf{V} = (\mathbf{v}_1 + \mathbf{v}_2)/2$ and the relative velocity $\mathbf{v}_r = \mathbf{v}_1 - \mathbf{v}_2$. The collision integral becomes

$$C(\Delta\chi) = \frac{n}{2}\int d^3v_r\,\rho_r(\mathbf{v_r},\mathbf{T})\int d\Omega_{\mathbf{k}'}\frac{d\sigma}{d\Omega_{\mathbf{k}'}}v_r\Delta\chi, \quad (35)$$

where $\Delta\chi$ now reads

$$\Delta\chi = \tfrac{1}{2}\mu\left(v_{r,z}'^2 - v_{r,y}'^2\right) - \tfrac{1}{2}\mu\left(v_{r,z}^2 - v_{r,y}^2\right) \quad (36)$$

and $n = (1/N)\int d^3r n(\mathbf{r})^2$. The velocity distribution ρ_r has the same functional form as ρ in Eq. (30) *except* that the molecular mass m is replaced by the reduced mass μ.

Rethermalization proceeds at a rate characterized by

$$\gamma = -\frac{1}{\langle\chi\rangle}\frac{d\langle\chi\rangle}{dt}. \quad (37)$$

Substituting in the above expressions and definitions, we therefore find

$$\alpha = \frac{n v_r\bar{\sigma}}{\gamma} = -\frac{2k_B(T_z - T_y)v_r\bar{\sigma}}{\langle v_r\sigma\Delta\chi\rangle}, \quad (38)$$

using the suggestive notation

$$\langle v_r\sigma\Delta\chi\rangle = \int d^3v_r\,\rho_r(\mathbf{v}_r,\mathbf{T})v_r\int d\Omega_{\mathbf{k}'}\frac{d\sigma}{d\Omega_{\mathbf{k}'}}\Delta\chi. \quad (39)$$

This integral vanishes linearly as $T_z - T_y \to 0$, so that the ratio in Eq. (38) remains well defined in this limit. The ratio α is in general a weakly dependent function of the temperature asymmetry T_z/T_y. It may, however, have a significant dependence on the polarization direction, owing to the anisotropy of the dipole-dipole interaction.

B. Anisotropy of rethermalization rate

The integrals in Eq. (39) required to compute α can in principle be done analytically, even for the dipolar cross sections. They are, however, somewhat cumbersome, so we present numerical results here. In this subsection we present results in the limit of a low initial anisotropy, i.e., the limit $T_z/T_y \approx 1$, and, for the sake of simplicity, assume that $T_x = T_y$. As a point of reference, we note that expression (38) correctly reduces to the results $\alpha = 2.5$ for s-wave collisions and $\alpha = 25/6 = 4.17$ for p-wave collisions.

For collisions of dipolar particles, anisotropy of the scattering cross section implies that the rethermalization constant α may depend on the direction of polarization. We therefore model a rethermalization experiment where energy transfers between the laboratory z and the laboratory y directions, but the direction $\hat{\mathcal{E}}$ of the polarizing electric field is inclined at an angle λ with respect to the z axis (Fig. 2). We consider separately the cases of identical fermions, identical bosons, and distinguishable particles.

For identical fermions, this result is presented in Fig. 3. The upper panel shows the value of α versus the tilt angle λ, revealing that the rethermalization rate varies by more than a factor of 2. For identical fermions, dipolar collisions are most effective at rethermalizing the gas (smallest α) when $\hat{\mathcal{E}}$ is at 45° with respect to the trap axis and least effective when $\hat{\mathcal{E}}$ is at 90° of 0° with respect to the trap axis.

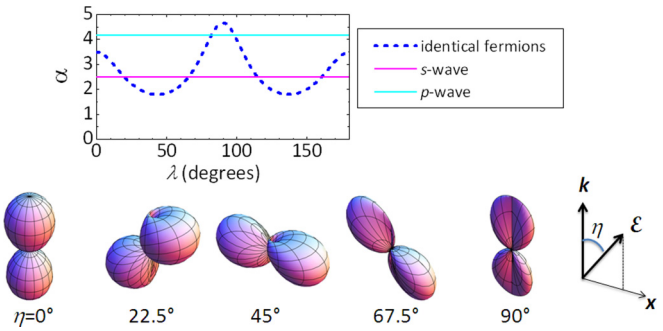

FIG. 3. (Color online) Upper panel: The parameter α, which characterizes the number of collisions per rethermalization as a function of the angle λ between the trap axis $\hat{z}$ and the quantization axis $\hat{\mathcal{E}}$. The result for dipolar collisions of indistinguishable fermions is shown in blue, while the cyan and magenta lines indicate α for s-wave and p-wave collisions, respectively. Lower panel: Differential cross sections for indistinguishable fermions as a function of scattering direction $\mathbf{k}'$. Each plot assumes incident direction $\mathbf{k}$ along the vertical, making an angle η with respect to $\hat{\mathcal{E}}$.

To understand the behavior of α, it is necessary to consider the differential cross section for various values of the angle η between the incident relative velocity and the quantization axis $\hat{\mathcal{E}}$. The lower panel in Figure 3 shows three-dimensional surface plots of the differential cross section as a function of the direction of the outbound scattering wave vector $\mathbf{k}'$. Each such figure is drawn for a different value of the angle η between the incident direction $\mathbf{k}$ (set as vertical in these diagrams) and the electric-field direction $\hat{\mathcal{E}}$.

Cross-dimensional rethermalization averages over many collisions with different incident angles η. The collisions that are most efficient at cross-dimensional rethermalization require two circumstances: first, the scattering cross section must be large, and second, the scattering must divert the direction of the incident velocity from either forward or backward scattering. For fermions, the largest cross section occurs for collisions incident at $\eta \approx 45°$ with respect to the electric field (Fig. 1). Moreover, these collisions are precisely the ones that tend to preferentially scatter at large angles (center lower panel in Fig. 3). By contrast, collisions that occur with incident direction $\eta \approx 0°$ or 90° with respect to the field not only scatter less (Fig. 1), but also preferentially scatter in the forward and backward directions (Fig. 3), and are not good at moving energy between dimensions.

Therefore, for an electric field tilted at an angle $\lambda = 45°$ with respect to the laboratory z axis, collisions should be relatively efficient at moving energy between radial and axial trap directions. For an electric field oriented at $\lambda = 0°$ or 90° with respect to the z axis, the most likely collisions, those with $\eta = 45°$, occur in an orientation that is less efficient at transferring energy between laboratory radial and laboratory axial directions. This circumstance is reflected in larger values of α for these tilt angles.

For identical bosons the situation is quite different, as shown in Fig. 4. Here the tilt angle $\lambda = 90°$ actually produces the most efficient rethermalization. The lower panel in Fig. 4 presents differential cross sections for various incident angles

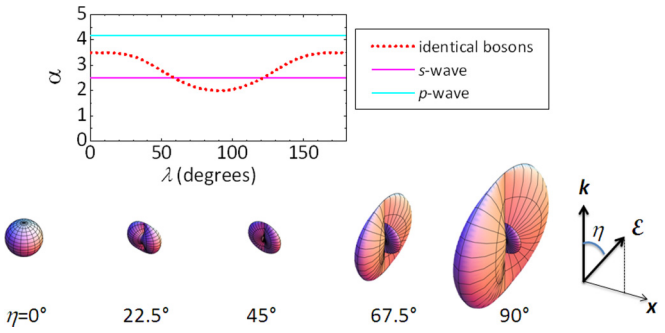

FIG. 4. (Color online) Upper panel: The parameter α, which characterizes the number of collisions per rethermalization as a function of the angle λ between the trap axis $\hat{z}$ and the quantization axis $\hat{\mathcal{E}}$. The result for dipolar collisions of indistinguishable bosons is shown in red, while the cyan and magenta lines indicate α for s-wave and p-wave collisions, respectively. Lower panel: Differential cross sections for indistinguishable bosons as a function of scattering direction $\mathbf{k}'$. Each plot assumes incident direction $\mathbf{k}$ along the vertical, making an angle η with respect to $\hat{\mathcal{E}}$.

η. Here the most likely collisions occur when $\eta = 90°$, and these collisions tend to scatter into the plane perpendicular to $\hat{\mathcal{E}}$. Thus if $\hat{\mathcal{E}}$ is aligned perpendicularly to the z axis ($\lambda = 90°$), collisions can shunt energy relatively efficiently between the axial direction and at least one radial direction in the trap. By contrast, if $\hat{\mathcal{E}}$ is aligned along $\hat{z}$ ($\lambda = 0°$), the relative velocity that originates in the x-y-plane tends to remain in this plane, whereas the relative velocity that originates along the z axis experiences isotropic scattering, but with a small cross section. In either event, cross-dimensional rethermalization occurs slowly.

Finally, for completeness we report the angular dependence of α for distinguishable particles in Fig. 5. Similarly to fermions, in this case the most efficient rethermalization occurs when the quantization axis $\hat{\mathcal{E}}$ lies at $\lambda = 45°$ with respect to

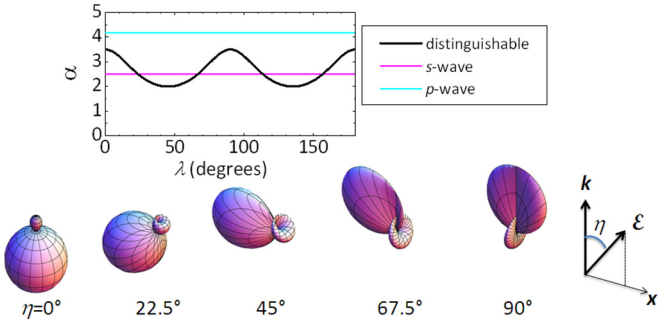

FIG. 5. (Color online) Upper panel: The parameter α, which characterizes the number of collisions per rethermalization as a function of the angle λ between the trap axis $\hat{z}$ and the quantization axis $\hat{\mathcal{E}}$. The result for dipolar collisions of distinguishable particles is shown in black, while the cyan and magenta lines indicate α for s-wave and p-wave collisions, respectively. Lower panel: Differential cross sections for distinguishable molecules as a function of scattering direction $\mathbf{k}'$. Each plot assumes incident direction $\mathbf{k}$ along the vertical, making an angle η with respect to $\hat{\mathcal{E}}$.

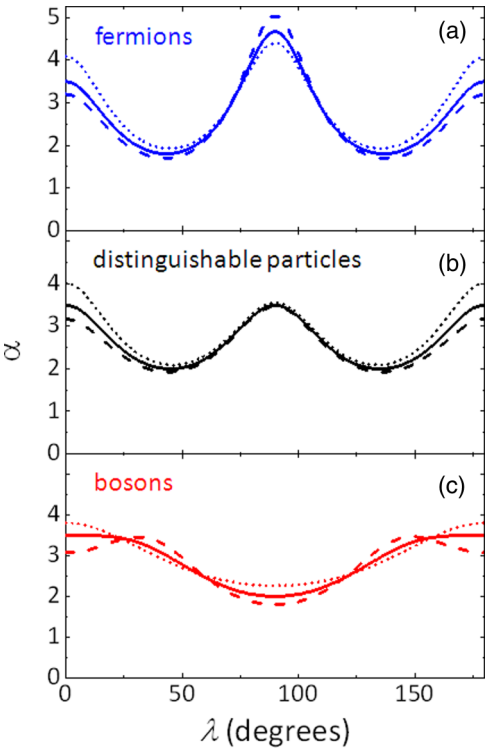

FIG. 6. (Color online) Dependence of α for cross-dimensional rethermalization on the initial temperature anisotropy for dipolar collisions of (a) identical fermions, (b) distinguishable particles, and (c) identical bosons. The solid line shows α in the limit of zero anisotropy, with the dashed line corresponding to $T_z = 2T_y$ and the dotted line to $T_z = 0.4T_y$.

the z axis, whereas, for $\hat{\mathcal{E}}$ either parallel or perpendicular to z, the scattering is primarily in the forward or backscattering direction and does not contribute strongly to rethermalization.

C. Dependence on the initial temperature imbalance

In extracting the elastic collision cross section from measurements of cross-dimensional rethermalization, it may be useful for experimenters to know the dependence of the rethermalization rate on the initial energy (or effective temperature) imbalance. As defined above, α is inversely proportional to the initial rethermalization rate and, hence, is sensitive to the initial value of the imbalance T_z/T_y. Figure 6 shows α versus the tilt angle λ for three values of the initial temperature imbalance $T_z/T_y = 0.4$, 1, and 2. For comparison, for s- or p-wave collisions, α decreases by 3% for $T_z/T_y = 2$ and increases by 4% for $T_z/T_y = 0.4$ compared to the limit of no imbalance ($T_z/T_y = 1$). As shown in Fig. 6, the effect of the initial temperature imbalance can be a few times stronger than this for dipolar collisions. This suggests that to accurately extract the elastic collision cross section from a measurement of cross-dimensional rethermalization, one would like to work in the limit of a small initial energy imbalance. Alternatively, measurements taken for a similar but opposite energy imbalance, namely, $T_z/T_y > 1$ and $T_z/T_y < 1$, could be averaged. In addition, in the case of

indistinguishable bosons, the shape of the α versus λ curve can qualitatively change depending on the temperature imbalance.

IV. RELATION TO THE PARTIAL-WAVE EXPANSION

Scattering of ultracold dipoles is commonly expressed in terms of a partial-wave expansion [15,19–25]. This is a useful thing to do, particularly for numerical calculations of scattering of realistic particles that include forces beyond the dipole-dipole interaction. In this section we examine the convergence of this expansion, noting that it is formally convergent but that this convergence may be quite slow owing to a discontinuity in the scattering amplitude in the forward scattering direction. We note that these remarks pertain only to the leading-order, real-valued scattering amplitude, as derived above in the first-order Born approximation.

A. The partial-wave expansion

The scattering amplitude in the first-order Born approximation can be expressed as a partial-wave expansion involving the spherical wave components of both the incoming and the outgoing waves,

$$f^{(1)}(\mathbf{k}',\mathbf{k}) = -\frac{2\pi}{k}\sum_{l'm'lm} i^{l'}Y^*_{l'm}(\hat{k}')\langle l'm'|T^{\rm Born}|lm\rangle i^{-l}Y_{lm}(\hat{k}), \tag{40}$$

where $T^{\rm Born} = i(S^{\rm Born} - I)$ is the transition matrix in terms of the usual scattering matrix S [26]. For dipolar scattering it is given by the product [4,15,22]

$$\langle l'm'|T^{\rm Born}|lm\rangle = -(ka_d)C^{(m)}_{l'l}\Gamma_{l'l} \tag{41}$$

in terms of the angular and radial integrals

$$C^{(m)}_{l'l} = (-1)^m\sqrt{(2l'+1)(2l+1)} \times \begin{pmatrix} l' & 2 & l \\ -m & 0 & m \end{pmatrix}\begin{pmatrix} l' & 2 & l \\ 0 & 0 & 0 \end{pmatrix}, \tag{42}$$

$$\Gamma_{l'l} = \begin{cases} \frac{4}{l(l+1)}, & l' = l, \\ \frac{4}{3l(l-1)}, & l' = l-2, \\ \frac{4}{3(l+1)(l+2)}, & l' = l+2. \end{cases} \tag{43}$$

(The expression for Γ corrects typographical errors in Ref. [15]). Within the first-order Born approximation, then, the scattering amplitude $f^{(1)}$ is appropriately proportional to a_d and independent of the wave number k.

Starting from the Born approximation, (10), the derivation in Sec. II directly expands the momentum-transfer part $e^{i\mathbf{q}\cdot\mathbf{r}}$ into partial waves. Alternatively, expanding both the ingoing and the outgoing plane waves separately into partial waves, the scattering amplitude reads

$$f^{(1)}(\mathbf{k}',\mathbf{k}) = -\frac{1}{2\pi}\int d^3r 4\pi\sum_{l'm'} i^{-l'}Y_{l'm'}(\hat{k}')j_{l'}(k'r)Y^*_{l'm'}(\hat{r}) \times\left(-\frac{2}{r^3}C_{20}(\hat{r})\right)4\pi\sum_{lm} i^{l}Y^*_{lm}(\hat{k})j_l(kr)Y_{lm}(\hat{r}). \tag{44}$$

Performing the integration over $\mathbf{r}$, one derives from this the partial wave series, (40). Alternatively one can separate radial and angular integrals, to get

$$f^{(1)}(\mathbf{k}',\mathbf{k}) = \frac{1}{\pi}(4\pi)^2\int_0^\infty r^2dr\frac{1}{r^3} \times\left[\sum_{l'lm} i^{-l'+l}Y^*_{l'm}(\hat{k}')j_{l'}(k'^r)C^{(m)}_{l'l}Y_{lm}(\hat{k})j_l(kr)\right]. \tag{45}$$

Using a generalized version of the familiar spherical harmonic addition theorem (Eq. (13) in Ref. [27]), the quantity in brackets can be rewritten

$$i^2\frac{1}{4\pi}\sqrt{\frac{4\pi}{2(2)+1}}Y_{20}(\hat{q})j_2(qr), \tag{46}$$

where $\mathbf{q} = \mathbf{k} - \mathbf{k}'$ is the familiar momentum transfer. The sum over partial-wave quantum numbers is therefore convergent for any given value of qr. Completing the integral as in Sec. II B yields the scattering amplitude, (17). We conclude that the partial-wave expansion and the explicit angular form of the scattering amplitude, (17), are formally equivalent.

B. Discontinuity of the scattering amplitude

In spite of its simple form, the unsymmetrized scattering amplitude, (17), contains a discontinuity when the scattered direction $\hat{k}'$ coincides with the incident direction $\hat{k}$. This fact is perhaps best illustrated by a simple example. Denote the two wave vectors in polar coordinates, $\hat{k} = (\theta_k,\phi_k)$ and $\hat{k}' = (\theta_{k'},\phi_{k'})$, as referred to the field axis. The limit of forward scattering, $\hat{k}' = \hat{k}$, can be reached in many ways, but two will suffice to show the discontinuity.

In the first limit we imagine that the azimuthal angles are equal, $\phi_{k'} = \phi_k$, and take the limit $\theta_k \to \theta_{k'}$. In this limit the angle θ_q that the vector $\mathbf{q} = \mathbf{k} - \mathbf{k}'$ makes with the field axis is given by $\theta_q = \theta_k + \pi/2$ (for $\theta_{k'} < \theta_k$). The forward scattering amplitude has the limit

$$\lim_{\theta_{k'}\to\theta_k} = -\tfrac{2}{3}[3\cos^2(\theta_k + \pi/2) - 1] = -\tfrac{2}{3}[3\sin^2(\theta_k) - 1], \tag{47}$$

a value that depends explicitly on the incident angle θ_k. Vice versa, one can take an alternative limit, where the polar angles are equal, $\theta_{k'} = \theta_k$, and let the azimulthal angles approach one another. In such a case, $\mathbf{q}$ is always perpendicular to the field axis, whereby $\theta_q = \pi/2$, and the scattering amplitude has the limit

$$\lim_{\phi_{k'}\to\phi_k} = -\tfrac{2}{3}[3\cos^2(\pi/2) - 1] = \tfrac{2}{3}, \tag{48}$$

independent on the incident direction. We conclude that the limit $\hat{k}' \to \hat{k}$ is, in general, ambiguous, depending on how this limit is taken.

Still, it is possible to assign a value to the forward scattering amplitude directly, by setting $\hat{k}' = \hat{k}$ directly in the partial-wave expansion, rather than taking a limit. Doing so in Eq. (40) yields the following. The sum over m, for fixed l' and l, can be

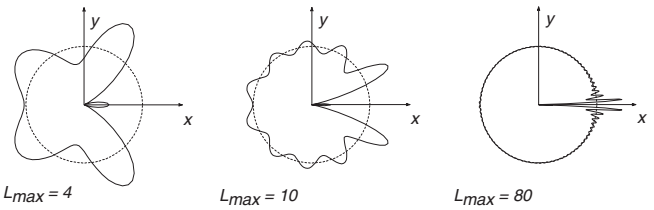

FIG. 7. Convergence of differential cross sections for various total numbers of partial waves $L_{\max}$ included in the sum, (40). The cross section $d\sigma/d\Omega_{\mathbf{k}'}$ versus the scattering direction $\mathbf{k}'$, for incident momentum $\mathbf{k} = \hat{x}$, with dipoles polarized out of the plane of the diagram. The solid line is the partial-wave sum, while the dashed circle is the analytic result $d\sigma/d\Omega_{\mathbf{k}'} = 4/9$.

evaluated from a spherical harmonic addition theorem [10]:

$$\sum_m (-1)^m Y^*_{l'm}(\hat{k}) \begin{pmatrix} l' & 2 & l \\ -m & 0 & m \end{pmatrix} Y_{lm}(\hat{k}) = \frac{\sqrt{(2l'+1)(2l+1)}}{4\pi} \begin{pmatrix} l' & 2 & l \\ 0 & 0 & 0 \end{pmatrix} C_{20}(\hat{k}). \quad (49)$$

This reduces the directional dependence to a single reduced spherical harmonic of the incident direction. The forward scattering amplitude then becomes

$$f(\hat{k},\hat{k}) = \frac{1}{2} C_{20}(\hat{k}) \sum_{l'l} i^{l'-l} (2l'+1)(2l+1) \begin{pmatrix} l' & 2 & l \\ 0 & 0 & 0 \end{pmatrix}^2 \Gamma_{l'l} \equiv \frac{1}{2} C_{20}(\hat{k}) \sum_{l'l} A_{l'l}, \quad (50)$$

which defines the shorthand notation $A_{l'l}$. All the factors defining $A_{l'l}$ have simple algebraic expressions [10], which vanish unless $l' = l,\ l \pm 2$. Inserting these expressions and accounting for $A_{00} = 0$, we group the terms as follows:

$$\sum_{l'l} A_{l'l} = A_{00} + A_{02} + A_{20} + \sum_{l=1}^{\infty} (A_{ll} + A_{l+2,l} + A_{l,l+2}) = -\frac{4}{3} + \sum_{l=1}^{\infty} \left[\frac{4(2l+1)}{(2l-1)(2l+3)} - \frac{4}{2l+3} \right] = \frac{4}{3}. \quad (51)$$

The forward scattering amplitude then becomes

$$f(\hat{k},\hat{k}) = \tfrac{2}{3} C_{20}(\hat{k}) = \tfrac{1}{3}(3\cos^2\theta_k + 1). \quad (52)$$

This discontinuity has implications for the convergence of the partial-wave expansion. We show an example of this convergence in Fig. 7. In this case we choose the unsymmetrized cross section $d\sigma/d\Omega_{\mathbf{k}'}$ and focus on scattering in the x-y plane, perpendicular to the polarization axis. Moreover, we set the scattering length $a = 0$. In this case, we see from Eq. (17) that, for any distinct directions $\hat{k}$ and $\hat{k}'$, both perpendicular to the field, $d\sigma/d\Omega_{\mathbf{k}'}$ is independent of the direction of scattering $\hat{k}'$ in this plane and has the value $d\sigma/d\Omega_{\mathbf{k}'} = 4/9$ in natural units. This cross section is shown as the dashed circle in all panels in Fig. 7.

The solid curves in each panel are numerical results that sum the Born series, (40), including partial waves up to some maximum value $L_{\max}$. The series is quite slow to converge. If only four partial waves are included, the cross section does not even come close, exhibiting a shape more like a butterfly than a circle. As more partial waves are included, the cross section conforms more closely to the correct, circular shape. There remain, however, large deviations in the forward scattering direction. These are the result of the discontinuity in this direction, which leads to a ringing familiar from the Gibbs phenomenon of Fourier expansion of discontinuous functions. It should be remarked that the numerical series evaluated in these figures does indeed yield the value $d\sigma/d\Omega_{k'} = 1/9$, as follows from Eq. (52) with $\theta_k = \pi/2$.

We conclude that, while the partial-wave version of the Born cross section is formally convergent, caution must be applied when numerically constructing differential cross sections for elastic scattering. This is particularly an issue when constructing cross sections for molecules with realistic interaction potentials that also have dipolar long-range behavior.

V. CONCLUSIONS

Reduction of the collision energy to the ultracold regime, as always, simplifies the theoretical description of scattering. For dipolar particles, however, this simplification does *not* reduce to isotropy of scattering, as it does for nondipolar particles. Rather, the differential cross section is a somewhat nontrivial function of both the incident and the scattered wave vectors, of the direction of polarization of the dipoles, and of the interplay among all three directions. To describe this scattering, it is useful to employ the direct expressions (17) and (18), rather than slowly converging partial-wave expansions.

The anisotropy that persists down to the ultracold regime has consequences for the rearrangement of energy due to collisions. We have shown that this anisotropy can have a profound influence on the rate of rethermalization of a gas taken out of equilibrium, since scattering at the required scattering angles can be made more or less favorable by adjusting the direction of the electric or magnetic field. Thus even a thermal, non-quantum-degenerate gas, at ultracold temperatures, may be expected to exhibit strong anisotropy if its constituent particles are dipolar.

ACKNOWLEDGMENT

This work was supported by the JILA NSF Physics Frontier Center, Grant No. 1125844.

[1] H. R. Sadeghpour, J. L. Bohn, M. J. Cavagnero, B. D. Esry, I. I. Fabrikant, J. Macek, and A. R. P. Rau, J. Phys. B **33**, R93 (2000).

[2] R. Shakeshaft, J. Phys. B **5**, L115 (1972). Strictly speaking, an isotropic $1/r^3$ potential posseses a phase shift with a logarithmic divergence as $k \to 0$. However, for a dipole-dipole interaction, the s-wave component of the interaction vanishes.

[3] T. F. O'Malley, Phys. Rev. **134**, A1188 (1964).

[4] I. I. Fabrikant, J. Phys. B **17**, 4223 (1984).

[5] T. Lahaye, J. Metz, B. Fröhlich, T. Koch, M. Meister, A. Griesmaier, T. Pfau, H. Saito, Y. Kawaguchi, and M. Ueda, Phys. Rev. Lett. **101**, 080401 (2008).
[6] M. Lu, N. Q. Burdick, S.-H. Youn, and B. L. Lev, Phys. Rev. Lett. **107**, 190401 (2011).
[7] M. Lu, N. Q. Burdick, and B. L. Lev, Phys. Rev. Lett. **108**, 215301 (2012).
[8] K. Aikawa, A. Frisch, M. Mark, S. Baier, A. Rietzler, R. Grimm, and F. Ferlaino, Phys. Rev. Lett. **108**, 210401 (2012).
[9] K. Aikawa, A. Frisch, M. Mark, S. Baier, R. Grimm, and F. Ferlaino, Phys. Rev. Lett. **112**, 010404 (2014).
[10] D. M. Brink and G. R. Satchler, *Angular Momentum*, 3rd ed. (Clarendon Press, Oxford, UK, 1993).
[11] J. P. Burke, Ph.D. thesis, University of Colorado Boulder (1999). Equation (8) differs slightly from this reference in that the angular integration is intended to be carried out over a complete 4π steradians.
[12] L. D. Landau and E. M. Lifshitz, *Quantum Mechanics (Non-relativistic Theory)*, 3rd ed. (Butterworth, Oxford, UK, 1977), Chap. XVII.
[13] R. H. Landau, *Quantum Mechanics II: A Second Course in Quantum Theory*, 2nd ed. (Wiley, New York, 1996), Chap. 5.
[14] L. Santos, G. V. Shlyapnikov, P. Zoller, and M. Lewenstein, Phys. Rev. Lett. **85**, 1791 (2000).
[15] J. L. Bohn, M. Cavagnero, and C. Ticknor, New J. Phys. **11**, 055039 (2009).
[16] C. R. Monroe, E. A. Cornell, C. A. Sackett, C. J. Myatt, and C. E. Wieman, Phys. Rev. Lett. **70**, 414 (1993).
[17] B. DeMarco, J. L. Bohn, J. P. Burke, M. Holland, and D. S. Jin, Phys. Rev. Lett. **82**, 4208 (1999).
[18] F. Reif, in *Fundamentals of Statistical and Thermal Physics* (McGraw–Hill, New York, 1965), pp. 525–529.
[19] M. Marinescu and L. You, Phys. Rev. Lett. **81**, 4596 (1998).
[20] S. Hansler, J. Werner, A. Griesmaier, P. O. Schmidt, A. Görlitz, T. Pfau, S. Giovanazzi, and K. Rzazewski, Appl. Phys. B **77**, 765 (2003).
[21] A. Derevianko, Phys. Rev. A **67**, 033607 (2003); **72**, 039901(E) (2005).
[22] K. Kanjilal, J. L. Bohn, and D. Blume, Phys. Rev. A **75**, 052705 (2007).
[23] C. Ticknor, Phys. Rev. Lett. **100**, 133202 (2008).
[24] D.-W. Wang, New J. Phys. **10**, 053005 (2008).
[25] V. Roudnev and M. Cavagnero, Phys. Rev. A **79**, 014701 (2009).
[26] N. F. Mott and H. S. Massey, *The Theory of Atomic Collisions*, 3rd ed. (Clarendon, Oxford, UK, 1965), Chap. XIV.
[27] M. Danos and L. C. Maximon, J. Math. Phys. **6**, 766 (1965).